

EXPERIMENTAL INVESTIGATION OF TWO-PHASE EJECTOR IN APPLICATION TO PROPANE REFRIGERATION SYSTEMS

**Jerzy Gagan^(a), Andrzej Pawluczuk^(a), Michał Łukaszuk^(a), Paweł Jakończuk^(a),
Kamil Śmierciew^(a), Dariusz Butrymowicz^(a), Sławomir Kubiczek^(b)**

(a) Białystok University of Technology, Faculty of Mechanical Engineering, Białystok, Poland,
d.butrymowicz@pb.edu.pl
(b) Frizo Ltd., Warszawa, Poland

ABSTRACT

Ejectors are mainly applied in refrigeration systems instead mechanical compressor, for increase the pressure from evaporation to condensation level. Recently, systems with ejector as a booster compressor were introduced, especially for CO₂ refrigeration systems. The application of ejector as a booster compressor allow for a significant extension of the range of available operating parameters of the heat pump, especially in the high-temperature region. The paper presents and discusses the experimental studied performed for the case of propane as a working fluid. The investigations of the four ejector geometries were carried out on a specially designed test stand. The tests were carried out for four different motive nozzle positions in relation to mixing chamber inlet (0.0 mm; 0.5 mm; 1.0 mm and 1.5 mm). Different discharge pressure were provided in the test. The working fluid used in the experiments was propane. The pressure and temperature distributions along the ejector will be shown. Based on the experimental investigation the velocity coefficients of motive nozzle and mixing chamber were determined. Keywords: two-phase ejector, propane, compressor-ejector systems, entrainment ratio

1. INTRODUCTION

Application of an two-phase ejector in compression refrigeration systems is a promising way to increase the system efficiency. Depending of the configuration ejector can operate as second step-compressor or a throttling device. In the first case ejector operates at high temperatures especially at suction chambers since ejector entrains vapour from compressor. The efficiency improvement results from the fact that less mechanical work is required to compress a liquid than to compress a vapour. Therefore, increasing the efficiency of the standard single-stage vapour compression cycle is achieved by reduction of mechanical compression at the expense of harnessing kinetic energy of a vapour in the ejector device. For the second case ejector operates at relatively low temperatures at suction chamber inlet since ejector sucks vapour from evaporator. In both cases ejector is feed by liquid from compressor. This configuration allows to reduce losses in the compression refrigeration and heat pump systems caused by the throttling process in the expansion valves by means of application of the liquid expansion instead of the isenthalpic throttling process.

The schematic diagram of vapour compression refrigeration device equipped with the two-phase ejector as a throttling device with the representation of the thermodynamic cycle in simple form is shown in Fig. 1. In the system presented in Fig. 1a liquid refrigerant (3) as the motive fluid expands in the motive nozzle and partly evaporate. In isentropic nozzle the expansion takes place along isentropic line 3-4s (see Fig. 1), while with the throttling valve expansion is represented by line 3-4d. In real motive nozzle expansion is represented by line 3-4. Motive fluid of high velocity emanating from the nozzle (4) causes suction of vapour from the evaporator (5) and compression in the mixing chamber (6) due to the momentum transfer. The additional compression of two-phase mixture takes place in the diffuser producing the inter-stage pressure in the system (7). Compressed two-phase mixture is separated in the separator, so the compressor sucks the vapour (1) while the liquid (8) flows to the evaporator through the throttling valve. In the system presented in Fig. 1b liquid refrigerant (7) is compressed by mechanical pump in order to produce high motive pressure (3). The suction chamber is connected with mechanical compressor (2). The compressor operates between the evaporation pressure and interstage pressure, while the ejector operates between interstage pressure and condensation pressure.

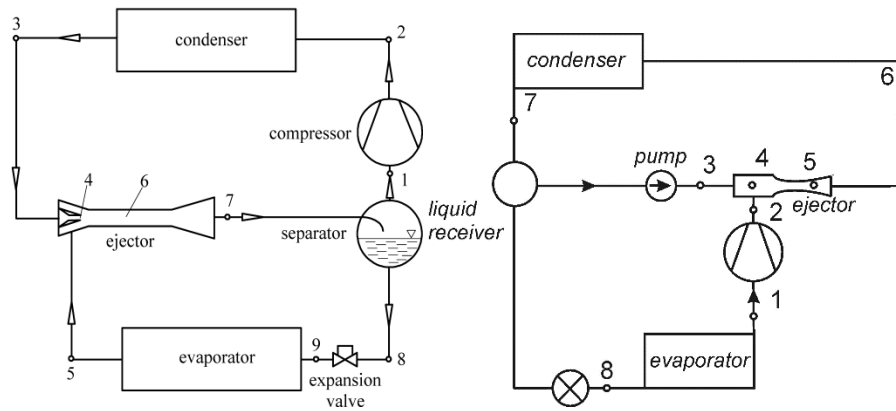


Figure 1. Schematic diagram of ejection-compression refrigeration device:
a) operating as booster compression device, and b) operating as second-step compressor

Recently significant improvement in modelling of two-phase ejector geometry has been obtained: Haider and Elbel (2021), Liu et al. (2022), de Souza et al. (2024). However, most of the research investigations are focused on carbon dioxide refrigeration systems and heat pumps with use of two-phase ejector as a booster compression device. Therefore, the developed modelling approaches to predict ejector geometry are rather based on experimental data for low pressure operation of the ejector. The control approaches of the performance of two-phase ejector for booster compression device have been developed recently by Gullo et al. (2020). Various applications of two-phase ejectors have been recently performed also for small capacity systems: Fingas et al. (2024), Sutthivirode and Thongtip (2024). The application of the two-phase ejector for hydrocarbon systems and low-GWP synthetic fluids has been recently studied: Fingas et al. (2024), Lu et al. (2023), de Souza et al. (2024). However, there is still a gap in knowledge concerning high pressure conditions operation of the two-phase ejector which is a motivation of the present experimental research.

2. RESEARCH DESCRIPTION

The test stand diagram is shown in Fig. 2. The system utilises propane as the working fluid. The compressor (Fig. 2. item b) is a semi-hermetic unit, BOCK EX-HG5/725-4S, manufactured according to ATEX requirements. Nominal cooling capacity of the compressor is 60 kW, the maximum discharge temperature is 140°C, and maximum discharge and inlet pressures are 28 bar and 19 bar, respectively. After passing through the oil separator (Castel 5540/9, item m), the vapour of the refrigerant discharges part of the heat of superheating in a water-cooled plate heat exchanger (c) before entering the secondary inlet of the ejector. Mass flow rate of the ejector secondary stream is measured by Endress+Hauser Promass 40E Coriolis-type mass flow meter (i). A bypass with a regulating valve is placed before the mass flow meter and allows to decrease the secondary stream flow rate of the ejector by releasing part of the vapour to the expansion valve (ALCO EX with EMERSON EC3-332 controller, item g). The condenser (e), evaporator (a), cooler (f) and primary stream heater (l) are also all plate heat exchangers. The cooler (f), placed after the condenser, facilitates an independent control of subcooling, regardless of condenser operation. Liquefied refrigerant is stored in a horizontal BITZER F302H 30 litre tank (item k), equipped with a safety valve. The primary stream of the ejector is pressurized by Hermetic CAM30/4 pump (h). The liquid refrigerant is drawn from the tank (k) and passed through the Endress+Hauser Promass 80E mass flow sensor (i), and heater (l) to bring the state of the refrigerant closer to the saturation state, to facilitate evaporation of the primary stream during expansion in the motive nozzle. After expansion, entraining the secondary stream, mixing and compression in the ejector, refrigerant enters the condenser or the liquid separator (j). The test stand in shown configuration allows the condenser to operate in two modes: when the liquid separator is in use, the condenser works in a similar way to condensers in vapour compressor systems, i.e. condensing the refrigerant from saturated vapour (not superheated) to liquid that is close to saturation state. When the liquid separator is bypassed, the condenser receives wet vapour.

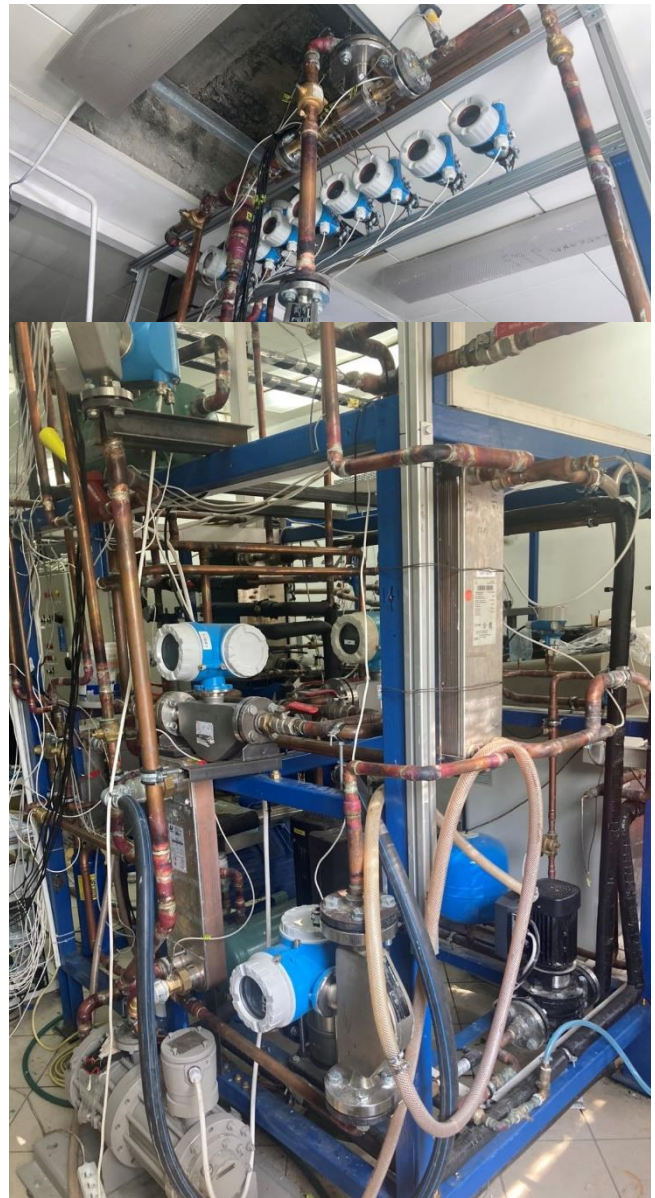
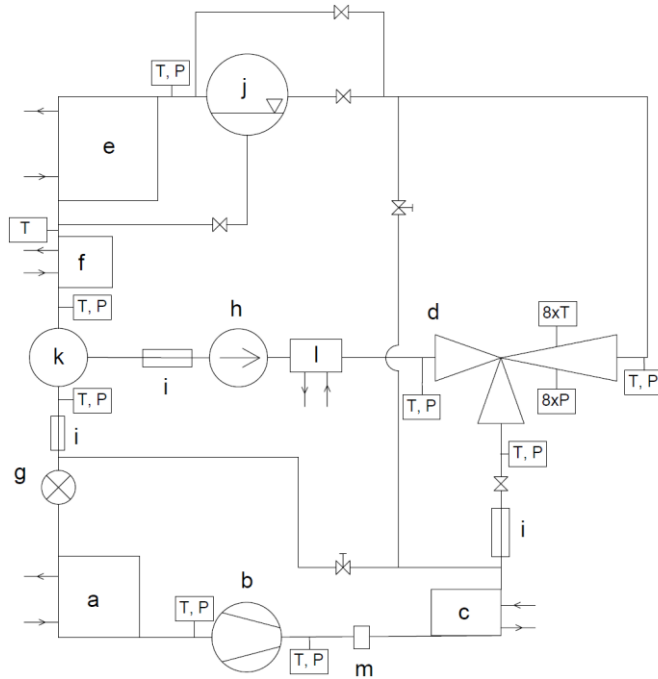


Figure 2. Test stand diagram (left side): a – evaporator; b – compressor; c – superheating discharge heat exchanger; d – tested ejector; e – condenser; f – cooler; g – expansion valve; h – ejector primary stream pump; i – mass flow meters; j – liquid separator; k – liquid refrigerant vessel; l – primary stream heater; m – oil separator; T, P – temperature and pressure sensors; photographs of the test stand at the left: the tested ejector with sensors (upper photo); general view of the system (lower photo).

The condenser (e) and cooler (f) are connected to a dry cooler STEFANI SDS 063/1C4DV with ethylene glycol as a working fluid. The glycol is pumped by Grundfoss TPE 32-230/2 RUUE inverter pump. The heat load loop for evaporator consists of two 24 kW Kospel EKCO.L1-24z electric boilers, Grundfoss CRNE 15-2 HQQE inverter pump and Galmet SGW200 heat exchanger (200 l tank, acting as the heat sink). The intermediate fluid in this loop is also ethylene glycol. In both condenser, and evaporator loops the mass flow rates of glycol are measured by Endress+Hauser Promass 40E mass flow meters. The primary stream heater (l) is driven by hot water heated by a separate electric boiler. The superheating discharge exchanger (c) is cooled by water. The last two exchangers operate only with liquid on the refrigerant side with known mass flow rate of propane, hence flow rates of water are not measured in these exchangers.

Data acquisition and control of the system is done by National Instruments hardware and LabView software. The

hardware consists of cDAQ-9189 chassis with modules: NI 9216 (RTD module), NI 9208 (16-channel Analogue Input, for pressure sensors), NI 9265 (4-channel Analog Input), NI PS-14 (24VDC power supply). Control application was built in NI Labview software. The application facilitates data recording, real-time view of all system parameters and remote control of system components, namely the compressor, pumps and expansion valve. The view of the main window of the data acquisition system is shown in Fig. 3.

Temperature and pressure sensor locations are shown on the diagram in Fig. 2. The ejector has additional 8 pairs of sensors along the mixing chamber and the diffuser to measure pressure and temperature distribution in the ejector. Additionally, temperatures are measured on all inlets and outlets of intermediate fluids in all heat exchangers. All of the temperature sensors, except for sensors in the ejector, are Czaki TP-207 $\varnothing 3$ mm PT100 units. Temperature distribution in the ejector is measured by Czaki TP-215 K $\varnothing 0.5$ mm thermocouples. Aplisens PC-28 sensors were utilised in the whole system, except for the ejector, where pressures are measured by 8 Endress+Hauser Cerabar M PMC51 sensors. All of the pressure and temperature measurements in the ejector are done in pairs, i.e. temperature and pressure is measured in each of all 8 locations.

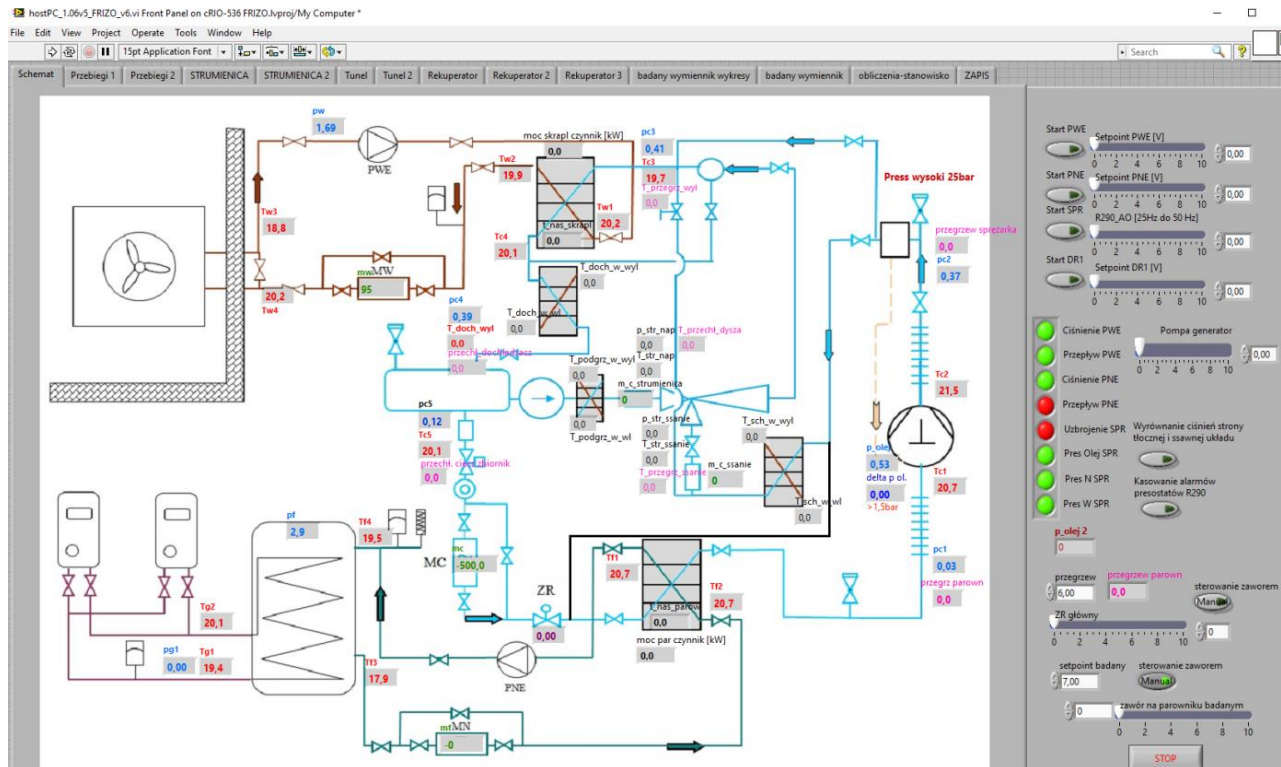


Figure 3. View of the main control panel with system diagram in NI LabView

Table 1. Geometry parameters of the tested ejectors, see Fig. 4.

Ejector geometry	$\frac{dn_t}{dn_{out}}$	α_{in}	α_{out}	$\frac{dm_{in}}{dm}$	β	$\frac{lm}{dm}$	$\frac{NXP}{dm}$	γ	dd [mm]
1	0.897	50°	10°	1.333	10°	10	0	10°	20
2	0.908	50°	10°	1.3	10°	10	0	10°	20

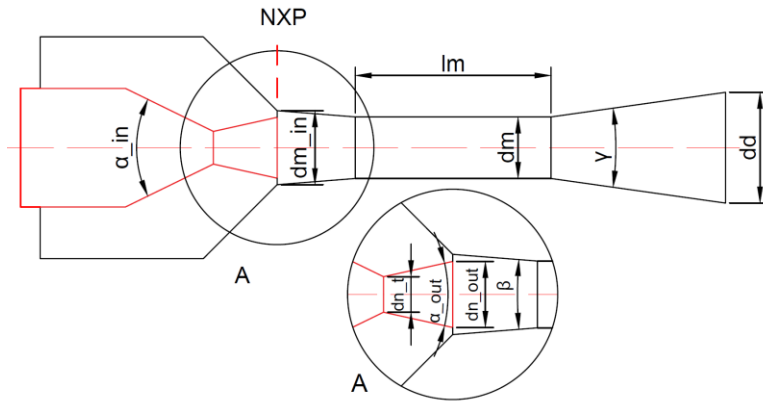


Figure 4. Main dimensions of the ejector.

3. EXPERIMENTAL RESULTS

Operating parameters of the tested ejectors covered motive liquid pressure range 20.7 to 22.3 bar, entrained vapour pressure range 16.0 to 18.6 bar, liquid subcooling of the motive liquid range 1.5 to 2.9 K, and entrained vapour superheating 0.8 to 5.7 K. Results of the 29 experimental runs are presented in Fig. 5 – Fig. 7.

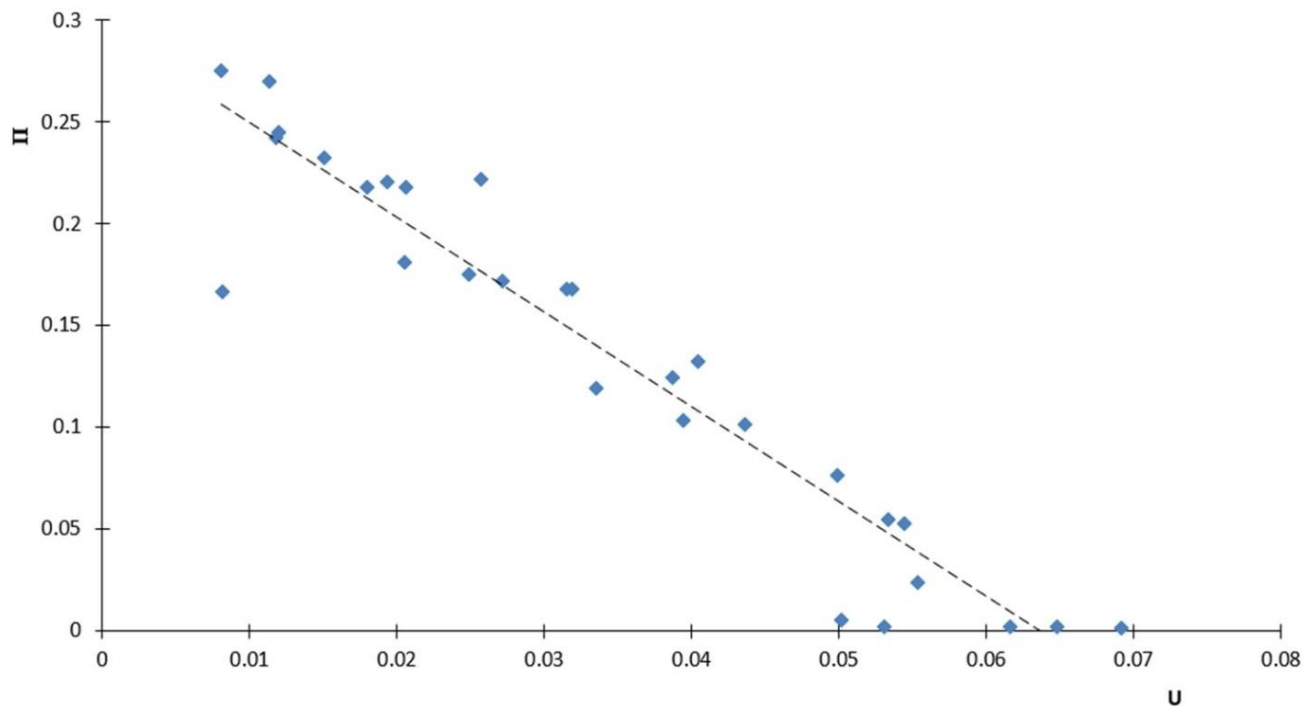


Figure 5. Performance line of the ejector as relationship between relationship of compression ratio Π and entrainment ratio U for ejector of Geometry 1.

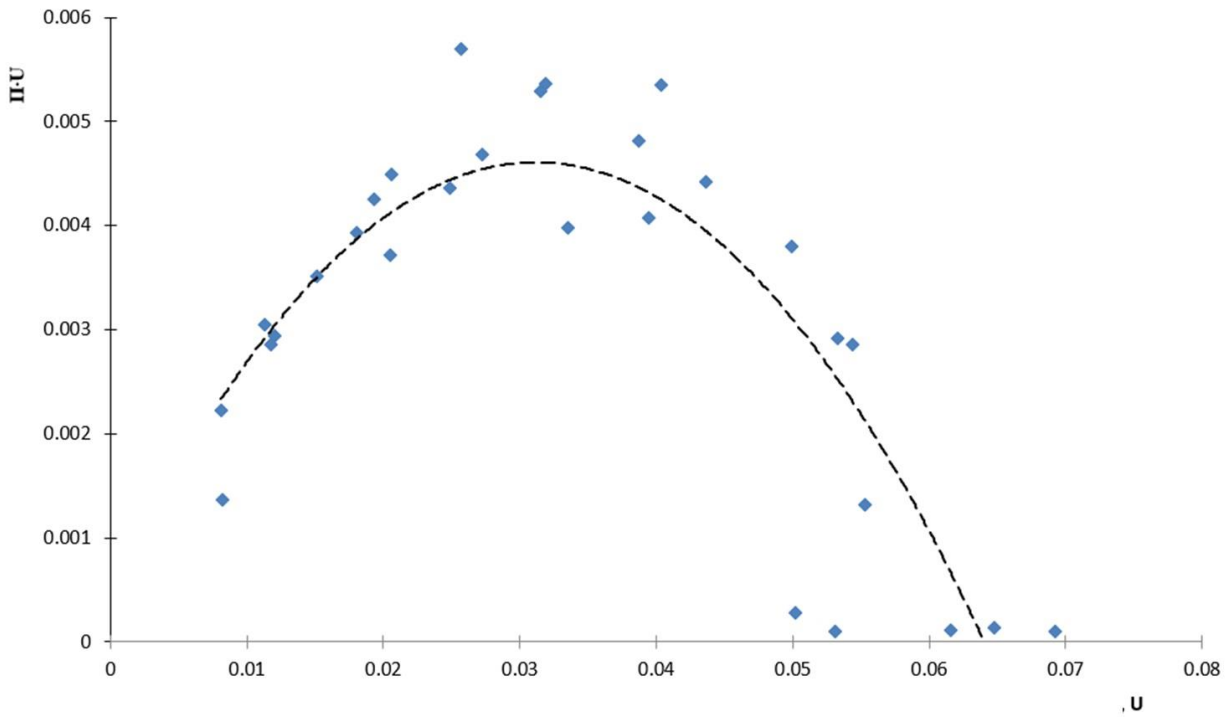


Figure 6. Relationship between product of compression ratio and entrainment ratio versus entrainment ratio for ejector of Geometry 1.

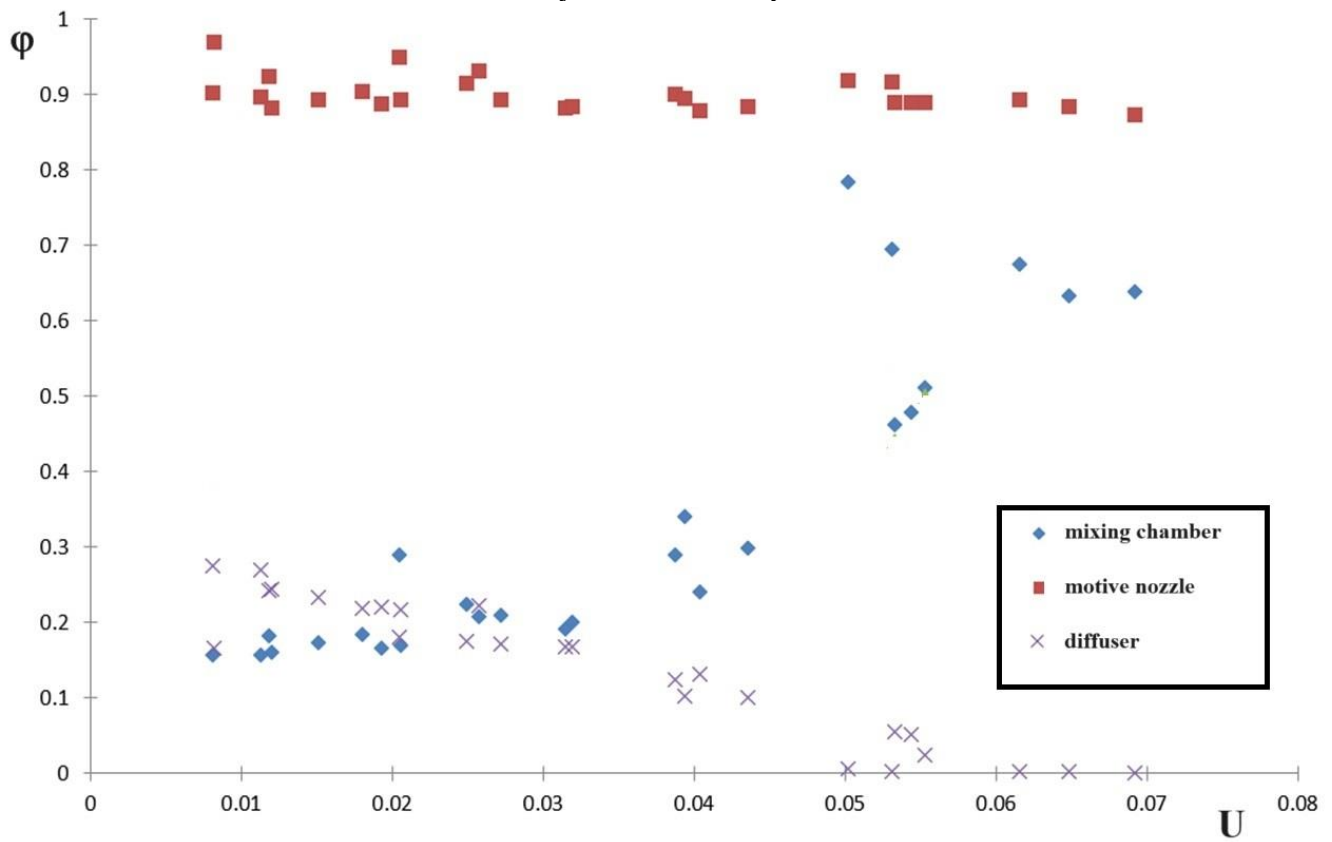


Figure 7. Relationship between velocity coefficients of the ejector components versus entrainment ratio for ejector of Geometry 1.

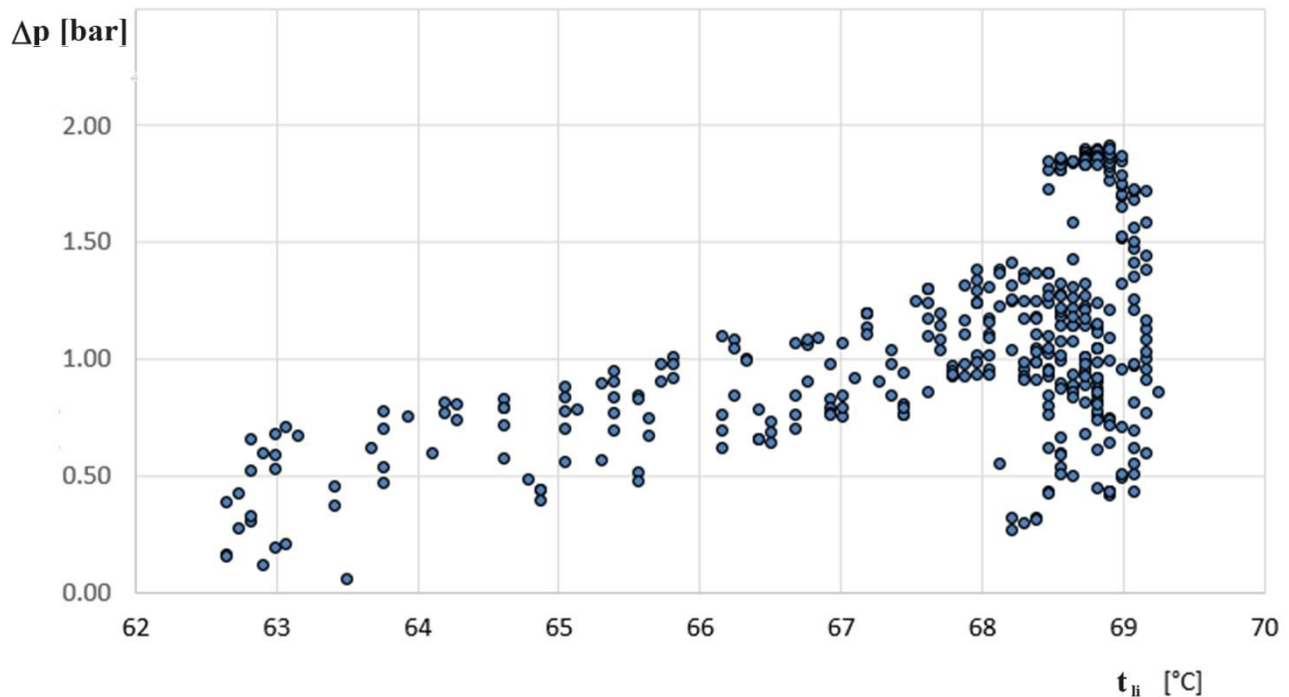


Figure 8. Relationship between pressure rise produced by the ejector versus motive temperature for ejector of Geometry 2; motive liquid pressure 24.6 bar, entrained vapour pressure 21.2 bar, entrained vapour superheating 8.5 K.

The obtained measurement values are presented in Fig. 5 to Fig. 8. In Fig. 5 there are presented all measurement points in the coordinate system: compression ratio versus mass entrainment ratio. As it is seen the points of all measurement series form one generalized linear characteristics. The efficiency of a two-phase jet in the context of applications in high-pressure conditions does not have a physically well-justified definition of efficiency, it can only be postulated that it will depend on the product of the pressure ratio and the mass entrainment ratio. The dependence of the product of these quantities versus the suction ratio is shown in Fig. 6, which demonstrates the optimal values of the entrainment ratio for the analyzed ejector operating under high-pressure conditions.

The tests obtained high values of the velocity coefficient of the motive nozzle, with the highest values of 0.95-0.97 obtained for critical flow conditions, at which a supersonic flow is formed at the nozzle outlet. For subcritical flow, the values of the speed coefficients of the driving nozzle range from 0.88 to 0.94.

Regarding the values of the mixing chamber velocity coefficients, for cases in which the mixing process took place in the outlet of the mixing chamber and partly in the diffuser, relatively high values of this coefficient are obtained, ranging from 0.86 to 0.92.

When calculating the resistance to two-phase flow in the mixing chamber, an approach was used using a two-phase multiplier for turbulent flow in both phases. Resistance correction factors vary from 0.16 to 0.78 and should be considered to be strongly dependent on both the pressure (determining the formation of two-phase flow structures) and the entrainment ratio. Due to the clear dependence of the pressure and the entrainment ratio (Fig. 5), it is therefore possible to consider the dependence of the resistance correction factor on only one variable, i.e. the suction ratio. The diffuser velocity coefficient varies from 0.40 to 0.53 and tends to increase with increasing suction ratio. This factor takes into account both mixing and flow resistance occurring in the diffuser.

The strong effect produced by motive liquid temperature on the compression ratio of the tested ejector is presented in Fig. 8. It is seen that motive liquid subcooling plays important role in efficient operation of the two-phase ejector.

4. CONCLUSIONS

Based on the presented results following conclusions can be drawn:

- a series of experimental tests were carried out and the operation of two-phase ejector under high-pressure conditions;
- the effect of compression ratio on available entrainment ratio has been demonstrated, the optimum entrainment ratio can be found on the basis of the experimental data;
- the range of the velocity coefficients for the motive nozzles, mixing chamber, and diffuser of the tested ejector have been reported;
- the effect of motive liquid temperature for the compression of the two-phase ejector has been demonstrated.

ACKNOWLEDGEMENTS

The research results presented in the paper were partially financed by the National Centre for Research and Development, Contract No. POIR.01.01.01-00-0239/21, and partially by the Project No. WZ/W_WM-IIM2_2023 supported by the Ministry of Science and Higher Education, Poland.

REFERENCES

- Fingas R., Haida M., Smolka J., Besagni G., Bodys J., Palacz M., Nowak A.J., Experimental analysis of the air-to-water ejector-based R290 heat pump system for domestic application, *Applied Thermal Engineering*, 236 (2024) 121800.
- Gullo P., Kærn M.R., Haida M., Smolka J., Elbel S., A review on current status of capacity control techniques for two-phase ejectors, *International Journal of Refrigeration*, 119 (2020) 64–79.
- Haider M., Elbel S., Development of ejector performance map for predicting fixed-geometry two-phase ejector performance for wide range of operating conditions, *International Journal of Refrigeration*, 28 (2021) 232–241.
- Liu Y., Yu M., Yu J., An improved 1-D thermodynamic modeling of small two-phase ejector for performance prediction and design, *Applied Thermal Engineering*, 204 (2022) 118006.
- Lu Y., Bai T., Yu J., Investigation on the influence of geometric parameters on two-phase ejector performance with R290, *International Journal of Refrigeration*, 156 (2023) 102–112.
- de Souza A.V., Barbieri P.E.L., Mól D.C.S., de Oliveira R.N., de Faria R.N., Thermodynamic analysis and optimization of a modified cascade refrigeration system using two-phase ejectors and low GWP fluids, *International Journal of Refrigeration*, 160 (2024) 54–64.
- Sutthivirode K., Thongtip T., Experimental investigation of a two-phase ejector installed into the refrigeration system for performance enhancement, *Energy Reports* 8 (2022) 7263–7273.